Evidence linking Arctic amplification to extreme weather in mid-latitudes

Jennifer A. Francis[1] and Stephen J. Vavrus[2]

[1] Arctic amplification (AA) – the observed enhanced warming in high northern latitudes relative to the northern hemisphere – is evident in lower-tropospheric temperatures and in 1000-to-500 hPa thicknesses. Daily fields of 500 hPa heights from the National Centers for Environmental Prediction Reanalysis are analyzed over N. America and the N. Atlantic to assess changes in north-south (Rossby) wave characteristics associated with AA and the relaxation of poleward thickness gradients. Two effects are identified that each contribute to a slower eastward progression of Rossby waves in the upper-level flow: 1) weakened zonal winds, and 2) increased wave amplitude. These effects are particularly evident in autumn and winter consistent with sea-ice loss, but are also apparent in summer, possibly related to earlier snow melt on high-latitude land. Slower progression of upper-level waves would cause associated weather patterns in mid-latitudes to be more persistent, which may lead to an increased probability of extreme weather events that result from prolonged conditions, such as drought, flooding, cold spells, and heat waves. **Citation:** Francis, J. A., and S. J. Vavrus (2012), Evidence linking Arctic amplification to extreme weather in mid-latitudes, *Geophys. Res. Lett.*, *39*, L06801, doi:10.1029/2012GL051000.

1. Introduction

[2] During the past few decades the Arctic has warmed approximately twice as rapidly as has the entire northern hemisphere [*Screen and Simmonds*, 2010; *Serreze et al.*, 2009], a phenomenon called Arctic Amplification (AA). The widespread warming resulted from a combination of increased greenhouse gases and positive feedbacks involving sea ice, snow, water vapor, and clouds [*Stroeve et al.*, 2012]. The area of summer sea ice lost since the 1980s would cover over 40% of the contiguous United States. As autumn freeze-up begins, the extra solar energy absorbed during summer in these vast new expanses of open water is released to the atmosphere as heat, thus raising the question of not *whether* the large-scale atmospheric circulation will be affected, but *how*? While global climate models project that the frequency and intensity of many types of extreme weather will increase as greenhouse gases continue to accumulate in the atmosphere [*Meehl et al.*, 2007], this analysis presents evidence suggesting that enhanced Arctic warming is one of the causes.

[3] Exploration of the atmospheric response to Arctic change has been an active area of research during the past decade. Both observational and modeling studies have identified a variety of large-scale changes in the atmospheric circulation associated with sea-ice loss and earlier snow melt, which in turn affect precipitation, seasonal temperatures, storm tracks, and surface winds in mid-latitudes [e.g., *Budikova*, 2009; *Honda et al.*, 2009; *Francis et al.*, 2009; *Overland and Wang*, 2010; *Petoukhov and Semenov*, 2010; *Deser et al.*, 2010; *Alexander et al.*, 2010; *Jaiser et al.*, 2012; *Blüthgen et al.*, 2012]. While it is understood that greenhouse-gas-induced tropospheric warming will cause an increase in atmospheric water content that is expected to fuel stronger storms and flooding [*Meehl et al.*, 2007], individual extreme weather events typically have a dynamical origin. Many of these events result from persistent weather patterns, which are typically associated with blocking and high-amplitude waves in the upper-level flow. Examples include the 2010 European and Russian heat waves, the 1993 Mississippi River floods, and freezing conditions in Florida during winter 2010–11. This study focuses on evidence linking AA with an increased tendency for a slower progression of Rossby waves in 500-hPa height fields that favor the types of extreme weather caused by persistent weather conditions, such as drought, flooding, heat waves, and cold spells in the northern hemisphere mid-latitudes.

2. Analysis and Results

[4] How does Arctic Amplification promote higher amplitude and slower moving waves? To address this question, output from the National Center for Environmental Prediction (NCEP)/National Center for Atmospheric Research (NCAR) Reanalysis (NRA) data set [*Kalnay et al.*, 1996] is used to assess changes in the atmosphere related to enhanced Arctic warming, and to investigate the effects of high-latitude change on mid-latitude patterns in 500 hPa heights. While direct comparisons of reanalysis to observations is problematic owing to a lack of independent measurements, *Archer and Caldeira* [2008] found that the upper-level circulation in the NRA is very similar to that of the European Centre for Medium-Range Weather Forecasts (ECMWF) Reanalysis (ERA-40), and *Bromwich et al.* [2007] found excellent agreement between surface pressure fields from these reanalyses in the Arctic after 1979, when assimilation of satellite data began. To reduce the possibility of spurious variability owing to differing data sources assimilated by the reanalysis, only fields from the post-satellite era are used.

[5] Following summers during recent decades with diminished Arctic sea ice, large fluxes of heat and moisture enter the lower atmosphere during fall and winter, which together with enhanced poleward fluxes of latent heat [*Alexeev*

[1] Institute of Marine and Coastal Sciences, Rutgers University, New Brunswick, New Jersey, USA.
[2] Center for Climatic Research, University of Wisconsin-Madison, Madison, Wisconsin, USA.
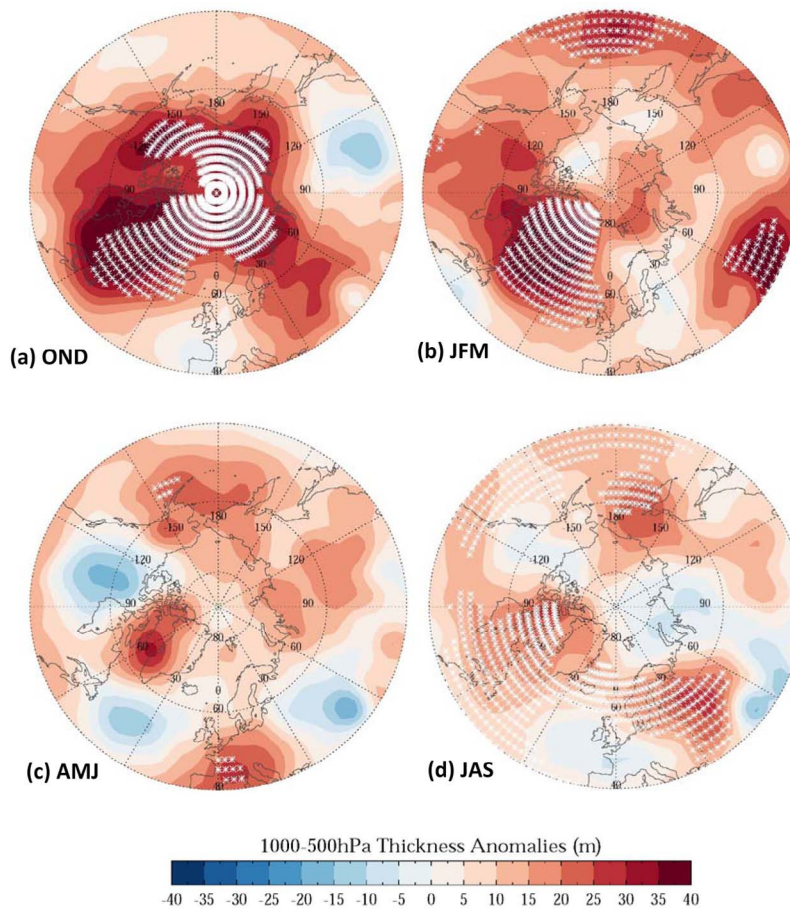
Figure 1. Seasonal anomalies in 1000-500 hPa thicknesses (m) north of 40°N during 2000–2010 relative to 1970–1999: (a) autumn (OND), (b) winter (JFM), (c) spring (AMJ), and (d) summer (JAS). White asterisks indicate significance with $p < 0.05$. Data are from the NCEP/NCAR Reanalysis.

et al., 2005], contribute to AA. This warming is clearly observable during autumn in near-surface air temperature anomalies in proximity to the areas of ice loss [Serreze et al., 2009]. The integrated lower-tropospheric warming is apparent in widespread anomalies in the vertical thickness of the layer between 1000 and 500 hPa, illustrated in Figure 1 for each season during 2000 to 2010 relative to the previous 30 years. During fall (Oct.–Dec.) statistically significant anomalies are apparent over much of the Arctic region, and during winter (Jan.–Mar.) a strong anomaly persists in the N. Atlantic and west of Greenland, along with positive areas at lower latitudes over Russia and the N. Pacific. Strong positive values during summer (Jun.–Sep.) occur mainly over high-latitude land areas, consistent with warmer, drier soils resulting from earlier snow melt [Brown et al., 2010]. Significant anomalies are absent in spring during recent years because heating that results from a reduced summer ice cover has dissipated and because high-latitude soils have not yet dried following snow melt.

[6] The differential warming of the Arctic relative to mid-latitudes is the key linking AA with patterns favoring persistent weather conditions in mid-latitudes. Two separate effects on upper-level characteristics are anticipated: weaker poleward thickness gradients cause slower zonal winds, and enhanced high-latitude warming causes 500 hPa heights to rise more than in mid-latitudes, which elongates the peaks of

ridges northward and increases wave amplitude. Both of these effects should slow eastward wave progression. Wave features in 500 hPa fields are analyzed from 1979 through 2010. The study focuses on the mid-latitudes of N. America and the N. Atlantic (140°W to 0°, Figure 2a), north of which the ice-loss has been substantial and atmospheric heating has been statistically significant (Figure 1). Fields of 500 hPa heights are selected for this analysis because they are constrained by observations from numerous radiosondes and satellite retrievals, they are relatively free from surface effects, and they capture upper-level wave patterns.

[7] Evidence supporting the first effect – zonal wind reduction – was identified in a previous study by Francis et al. [2009], who found that poleward thickness gradients were weaker over the N. Atlantic and N. Pacific in summers with less sea ice than normal, and that the weakening persisted well into the following spring. This tendency is also clearly evident over the present study region, as shown in the time series of 1000-500 hPa thickness differences between a high-latitude region (80–60°N) and low-latitude region (50–30°N) for each season (Figure 3, left). Since the late 1980s when rapid ice loss and enhanced warming began, poleward thickness differences have decreased in all seasons, especially during fall and winter (~10% with > 95% confidence in fall trend).
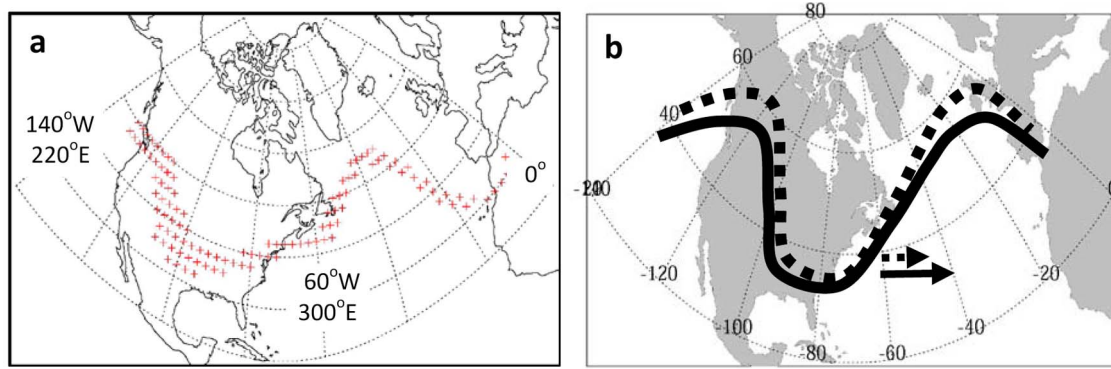
Figure 2. Region of study: 140°W to 0°. (a) Asterisks illustrate an example of a selected range of 500 hPa heights used in the analysis. (b) Schematic of ridge elongation (dashed vs. solid) in upper-level heights caused by enhanced warming in Arctic relative to mid-latitudes. Higher amplitude waves progress eastward more slowly, as indicated by arrows.

[8] The strength of the poleward thickness gradient determines the speed of upper-level zonal winds. As the gradient has decreased with a warming Arctic, the upper-level zonal winds during fall have also weakened since 1979 (Figure 3, right), with a total reduction of about 14% (>95% confidence). Winter winds are more variable but exhibit a steady decline since the early 1990s. When zonal wind speed decreases, the large-scale Rossby waves progress more slowly from west to east, and weaker flow is also associated with higher wave amplitudes [*Palmén and Newton*, 1969]. Slower progression of upper-level waves causes more persistent weather conditions that can increase the likelihood of certain types of extreme weather, such as drought, prolonged precipitation, cold spells, and heat waves. Previous studies support this idea: weaker zonal-mean, upper-level wind is associated with increased atmospheric blocking events in the northern hemisphere [*Barriopedro and Garcia-Herrera*, 2006] as well as with cold-air outbreaks in the western U.S. and Europe [*Thompson and Wallace*, 2001; *Vavrus et al.*, 2006].

[9] The second effect – ridge elongation – is also expected in response to larger increases in 500-hPa heights at high latitudes than at mid-latitudes. This effectively stretches the peaks of ridges northward, as illustrated schematically in Figure 2b, and further augments the wave amplitude. Higher amplitude waves also tend to progress more slowly. Evidence of this mechanism is investigated by selecting a narrow range of 500 hPa heights for each season that captures the daily wave pattern in the height field. The following ranges were used for fall: 5600 m $\pm$ 50 m, winter: 5400 m $\pm$ 50 m, and summer: 5700 m $\pm$ 50 m. The example in Figure 2a illustrates an "isoheight" represented by the selected gridpoints over the study region on a typical day, which are then analyzed to reveal changes in 500 hPa patterns over time.

[10] First row of Figures 4a–4c presents time series of the seasonally averaged maximum latitude of daily isoheights (corresponding to peaks of ridges) for fall, winter, and summer. Spring is not shown because high-latitude thickness anomalies are not statistically different from mean conditions. The steady northward progression of ridge peaks supports the hypothesis that AA is contributing to ridge elongation; confidence in these trends exceeds 99%. The fall plot also presents the time series of September sea ice extent (reversed scale, Spearman's correlation = −0.71) derived from passive microwave satellite information (obtained from the National Snow and Ice Data Center, http://nsidc.org/data/docs/noaa/g02135_seaice_index/ [*Fetterer et al.*, 2002]). The winter
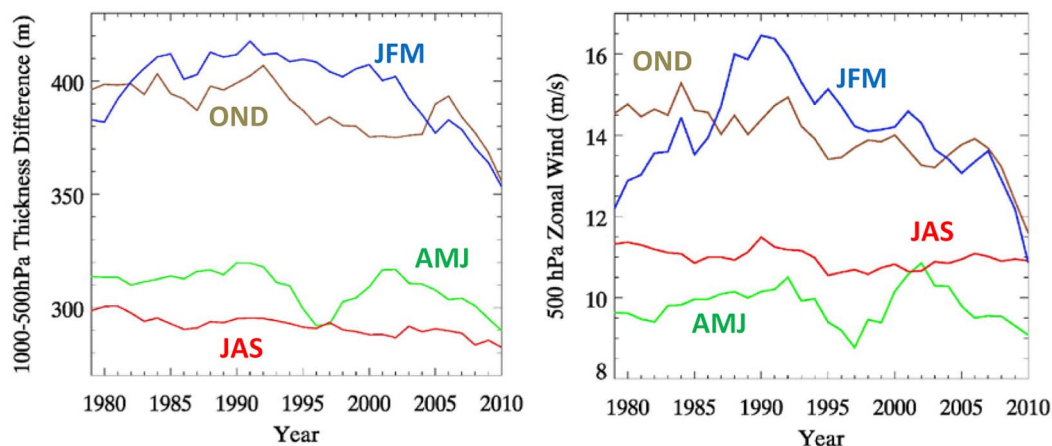
Figure 3. (left) Time series of seasonal 1000–500 hPa thickness differences between 80–60°N and 50–30°N over the study region (140°W to 0°). (right) Seasonal zonal mean winds at 500 hPa between 60–40°N over the study region. Seasons are labeled. Data obtained from the NCEP/NCAR reanalysis, http://www.esrl.noaa.gov/psd.
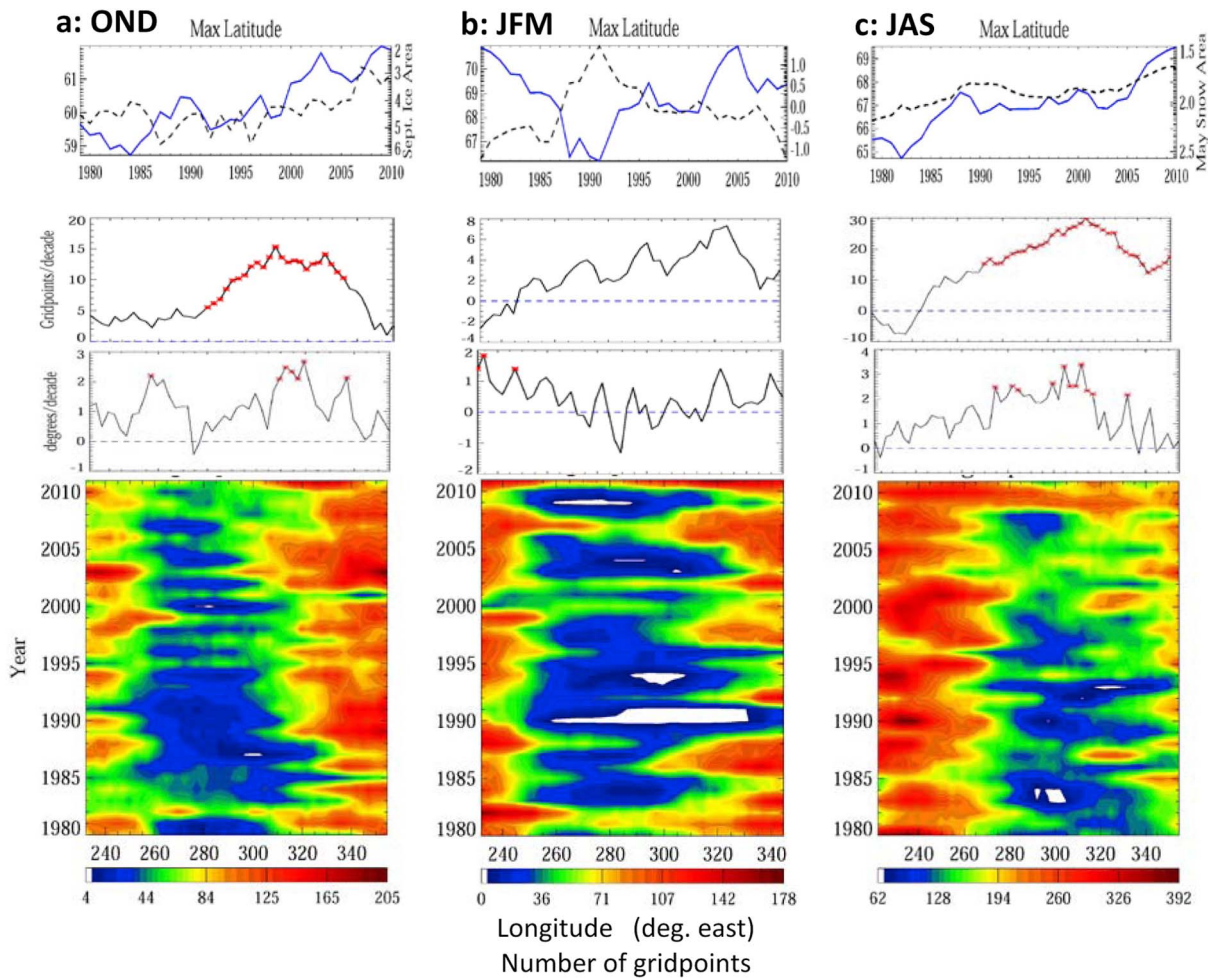
Figure 4. First row shows time series of maximum latitude of ridge peaks during (a) fall, (b) winter, and (c) summer from 1979 to 2010. A running 5-year box-car smoother was applied. The dotted line in fall is the time series of September-mean sea ice area (reversed axis, $\times 10^6$ km^2); in winter the JFM Arctic Oscillation Index, and in summer the northern hemisphere snow cover for May (reversed axis, $\times 10^7$ km^2). Second row is trends in the number of gridpoints that are located north of 50°N (60°N for winter) vs. longitude for each season. Red asterisks indicate significance at a 90% confidence level, the zero line is dashed blue. Third row is the same as the second row, but for wave amplitude (deg./decade). Fourth row (Hovmöller diagrams) presents time/longitude variations in the numbers of gridpoints located north of 50°N (60°N winter) with 500 hPa heights in the ranges of 5600, 5400, and 5700 m ($\pm$50 m) for each season, respectively. See text for details.

Arctic Oscillation index [*Thompson and Wallace*, 2001] appears in the winter panel, with a correlation of −0.65. Along with the summer panel is plotted the time series for the northern hemisphere snow cover for May (obtained from the Rutgers University Global Snow Lab, http://climate.rutgers.edu/snowcover [*Ghatak et al.*, 2010]). The two curves are strongly correlated with r = −0.88, suggesting the northward elongation of ridge peaks may be a response to enhanced warming over high-latitude land owing to earlier snow melt and warming soil [*Jaeger and Seneviratne*, 2011].

[11] Could this poleward shift be explained by the observed migration of the entire height field, rather than only the ridge peaks, in response to increasing greenhouse gases, as reported by *Seidel and Randel* [2007]? The analysis presented in the fourth row of Figures 4a–4c sheds light on this question. Hovmöllor diagrams present time/longitude contours that illustrate the preferred locations and time evolution of the number of gridpoints in each selected 500 hPa isopleth that are located north of 50°N (i.e., peaks of

ridges) during autumn and summer, and north of 60°N during winter. Related to these Hovmöllors is the second row of Figure 4, which displays trends in the number of these gridpoints, indicating which longitudes have experienced a change in ridging over the past three decades. Finally, the third row of plots presents the corresponding trends in wave amplitude, calculated as the difference between the maximum and minimum latitude of the isopleths along each longitude for each season and year. This difference calculation also helps mitigate any systematic bias in the reanalysis height field. While the significance of the trends in ridge points or wave amplitude at any one longitude often falls short of a 90% confidence level (marked with red asterisks), the probability is near zero (p $< 10^{-5}$) that the population of positive trends in ridging and amplitudes for all longitudes can be random.

[12] The Hovmöllor diagrams exhibit the clear geographic preferences of ridge axes during each season. In fall they tend to align over western N. America and the eastern

N. Atlantic. Trends in ridge gridpoints (second row) are positive across the region, with largest values over the entire N. Atlantic. Corresponding trends in wave amplitude (third row) are also positive at most longitudes, with the largest increases in the central U.S. and central N. Atlantic. These tendencies favor warmer, more persistent conditions along the N. American east coast and in the N. Atlantic, and may have contributed to the dramatic increase in maximum temperature extremes in those areas during fall, as shown in the Climate Extreme Index (available from NOAA's National Climate Data Center, http://www.ncdc.noaa.gov/extremes/cei/ [*Gleason et al.*, 2008]).

[13] During winter the preferred longitudinal positioning of ridges is similar to those in autumn, and ridging trends are again positive at most longitudes. While wave amplitude trends are less uniform, significant increases appear particularly over the Rocky Mountains, which is consistent with more persistent patterns that may have contributed to reduced mountain snowpacks in recent decades [*Mote*, 2006]. The Hovmöllor plot for summer shows that ridging occurs predominantly over central and western N. America, but the largest increases in ridge gridpoints (second row) have occurred over the eastern N. Atlantic. Trends in wave amplitude are positive nearly everywhere, particularly from the east coast of N. America across the N. Atlantic. Increased ridging and higher wave amplitudes over the Atlantic may have contributed to unprecedented surface melt in Greenland during recent years [*Tedesco et al.*, 2011] as well as to recent heat-waves in western Europe [*Jaeger and Seneviratne*, 2011].

3. Conclusions

[14] In summary, the observational analysis presented in this study provides evidence supporting two hypothesized mechanisms by which Arctic amplification – enhanced Arctic warming relative to that in mid-latitudes – may cause more persistent weather patterns in mid-latitudes that can lead to extreme weather. One effect is a reduced poleward gradient in 1000-500 hPa thicknesses, which weakens the zonal upper-level flow. According to Rossby wave theory, a weaker flow slows the eastward wave progression and tends to follow a higher amplitude trajectory, resulting in slower moving circulation systems. More prolonged weather conditions enhance the probability for extreme weather due to drought, flooding, cold spells, and heat waves. The second effect is a northward elongation of ridge peaks in 500 hPa waves, which amplifies the flow trajectory and further exacerbates the increased probability of slow-moving weather patterns. While Arctic amplification during autumn and winter is largely driven by sea-ice loss and the subsequent transfer of additional energy from the ocean into the high-latitude atmosphere, the increasing tendency for high-amplitude patterns in summer is consistent with enhanced warming over high-latitude land caused by earlier snow melt and drying of the soil. Enhanced 500-hPa ridging observed over the eastern N. Atlantic is consistent with more persistent high surface pressure over western Europe. This effect has been implicated as contributing to record heat waves in Europe during recent summers [*Jaeger and Seneviratne*, 2011].

[15] Can the persistent weather conditions associated with recent severe events such as the snowy winters of 2009/2010 and 2010/2011 in the eastern U.S. and Europe, the historic drought and heat-wave in Texas during summer 2011, or record-breaking rains in the northeast U.S. of summer 2011 be attributed to enhanced high-latitude warming? Particular causes are difficult to implicate, but these sorts of occurrences are consistent with the analysis and mechanism presented in this study. As the Arctic sea-ice cover continues to disappear and the snow cover melts ever earlier over vast regions of Eurasia and North America [*Brown et al.*, 2010], it is expected that large-scale circulation patterns throughout the northern hemisphere will become increasingly influenced by Arctic Amplification. Gradual warming of the globe may not be noticed by most, but everyone – either directly or indirectly – will be affected to some degree by changes in the frequency and intensity of extreme weather events as greenhouse gases continue to accumulate in the atmosphere. Further research will elucidate the types, locations, timing, and character of the weather changes, which will provide valuable guidance to decision-makers in vulnerable regions.

References

Alexander, M. A., R. Tomas, C. Deser, and D. M. Lawrence (2010), The atmospheric response to projected terrestrial snow changes in the late 21st century, *J. Clim.*, *23*, 6430–6437, doi:10.1175/2010JCLI3899.1.

Alexeev, V. A., P. L. Langen, and J. R. Bates (2005), Polar amplification of surface warming on an aquaplanet in ghost forcing experiments without sea ice feedbacks, *Clim. Dyn.*, *24*, 655–666, doi:10.1007/s00382-005-0018-3.

Archer, C. L., and K. Caldeira (2008), Historical trends in the jet streams, *Geophys. Res. Lett.*, *35*, L08803, doi:10.1029/2008GL033614.

Barriopedro, D., and R. Garcia-Herrera (2006), A climatology of Northern Hemisphere blocking, *J. Clim.*, *19*, 1042–1063, doi:10.1175/JCLI3678.1.

Blüthgen, J., R. Gerdes, and M. Werner (2012), Atmospheric response to the extreme Arctic sea ice conditions in 2007, *Geophys. Res. Lett.*, *39*, L02707, doi:10.1029/2011GL050486.

Bromwich, D. H., R. L. Fogt, K. I. Hodges, and J. E. Walsh (2007), A tropospheric assessment of the ERA-40, NCEP, and JRA-25 global reanalyses in the polar regions, *J. Geophys. Res.*, *112*, D10111, doi:10.1029/2006JD007859.

Brown, R., C. Derksen, and L. Wang (2010), A multi-dataset analysis of variability and change in Arctic spring snow cover extent, 1967–2008, *J. Geophys. Res.*, *115*, D16111, doi:10.1029/2010JD013975.

Budikova, D. (2009), Role of Arctic sea ice in global atmospheric circulation: A review, *Global Planet. Change*, *68*(3), 149–163, doi:10.1016/j.gloplacha.2009.04.001.

Deser, C., R. Tomas, M. Alexander, and D. Lawrence (2010), The seasonal atmospheric response to projected Arctic sea ice loss in the late 21st century, *J. Clim.*, *23*, 333–351, doi:10.1175/2009JCLI3053.1.

Fetterer, F., K. Knowles, W. Meier, and M. Savoie (2002), Sea ice index, digital media, Natl. Snow and Ice Data Cent., Boulder, Colo.

Francis, J. A., W. Chan, D. Leathers, J. R. Miller, and D. E. Veron (2009), Winter Northern Hemisphere weather patterns remember summer Arctic sea ice extent, *Geophys. Res. Lett.*, *36*, L07503, doi:10.1029/2009GL037274.

Ghatak, D., A. Frei, G. Gong, J. Stroeve, and D. Robinson (2010), On the emergence of an Arctic amplification signal in terrestrial Arctic snow extent, *J. Geophys. Res.*, *115*, D24105, doi:10.1029/2010JD014007.

Gleason, K. L., J. H. Lawrimore, D. H. Levinson, T. R. Karl, and D. J. Karoly (2008), A revised U.S. climate extremes index, *J. Clim.*, *21*, 2124–2137, doi:10.1175/2007JCLI1883.1.

Honda, M., J. Inoue, and S. Yamane (2009), Influence of low Arctic sea-ice minima on anomalously cold Eurasian winters, *Geophys. Res. Lett.*, *36*, L08707, doi:10.1029/2008GL037079.

Jaeger, E. B., and S. I. Seneviratne (2011), Impact of soil moisture-atmosphere coupling on European climate extremes and trends in a regional climate model, *Clim. Dyn.*, *36*, 1919–1939, doi:10.1007/s00382-010-0780-8.

Jaiser, R., K. Dethloff, D. Handorf, A. Rinke, and J. Cohen (2012), Impact of sea ice cover changes on the Northern Hemisphere atmospheric winter circulation, *Tellus, Ser. A*, *64*, 11595, doi:10.3402/tellusa.v64i0.11595.

Kalnay, E., et al. (1996), The NCEP/NCAR 40-year reanalysis project, *Bull. Am. Meteorol. Soc.*, *77*, 437–471, doi:10.1175/1520-0477(1996)077<0437:TNYRP>2.0.CO;2.

Meehl, G. A., et al. (2007), Global climate projections, in *Climate Change 2007: The Physical Science Basis. Contribution of Working Group I to the Fourth Assessment Report of the Intergovernmental Panel on Climate Change*, edited by S. Solomon et al., pp. 747–845, Cambridge Univ. Press, Cambridge, U. K.

Mote, P. W. (2006), Climate-driven variability and trends in mountain snowpack in western North America, *J. Clim.*, *19*, 6209–6220, doi:10.1175/JCLI3971.1.

Overland, J. E., and M. Wang (2010), Large-scale atmospheric circulation changes are associated with the recent loss of Arctic sea ice, *Tellus, Ser. A*, *62*, 1–9, doi:10.1111/j.1600-0870.2009.00421.x.

Palmén, E., and C. W. Newton (1969), *Atmospheric Circulation Systems*, *Int. Geophys. Ser.*, vol. 13, Academic, New York.

Petoukhov, V., and V. A. Semenov (2010), A link between reduced Barents-Kara sea ice and cold winter extremes over northern continents, *J. Geophys. Res.*, *115*, D21111, doi:10.1029/2009JD013568.

Screen, J. A., and I. Simmonds (2010), The central role of diminishing sea ice in recent Arctic temperature amplification, *Nature*, *464*, 1334–1337, doi:10.1038/nature09051.

Seidel, D. J., and W. J. Randel (2007), Recent widening of the tropical belt: Evidence from tropopause observations, *J. Geophys. Res.*, *112*, D20113, doi:10.1029/2007JD008861.

Serreze, M. C., A. P. Barrett, J. C. Stroeve, D. N. Kindig, and M. M. Holland (2009), The emergence of surface-based Arctic amplification, *Cryosphere*, *3*, 11–19, doi:10.5194/tc-3-11-2009.

Stroeve, J. C., M. C. Serreze, M. M. Holland, J. E. Kay, J. Maslanik, and A. P. Barrett (2012), The Arctic's rapidly shrinking sea ice cover: A research synthesis, *Clim. Change*, *110*, 1005–1027, doi:10.1007/s10584-011-0101-1.

Tedesco, M., X. Fettweis, M. R. van den Broeke, R. S. W. van de Wal, C. J. P. P. Smeets, W. J. van de Berg, M. C. Serreze, and J. E. Box (2011), Record summer melt in Greenland in 2010, *Eos Trans. AGU*, *92*(15), 126, doi:10.1029/2011EO150002.

Thompson, D. W., and J. M. Wallace (2001), Regional climate impacts of the Northern Hemisphere annular mode, *Science*, *293*, 85–89, doi:10.1126/science.1058958.

Vavrus, S., J. E. Walsh, W. L. Chapman, and D. Protis (2006), The behavior of extreme cold air outbreaks under greenhouse warming, *Int. J. Climatol.*, *26*, 1133–1147, doi:10.1002/joc.1301.

J. A. Francis, Institute of Marine and Coastal Sciences, Rutgers University, 71 Dudley Rd., New Brunswick, NJ 08901, USA. (francis@imcs.rutgers.edu)

S. J. Vavrus, Center for Climatic Research, University of Wisconsin-Madison, 1225 West Dayton St., Madison, WI 53706, USA.